



CRYSTAL GROWTH IN SOLUTION AND CHARACTERIZATION OF RUBIDIUM SULFATE SINGLE CRYSTALS DOPED WITH L-LEUCINE

Gershom Jebaraj P.*¹, Sivashankar V.²

¹Reg. No.: 18231282131041, Crystal Research Centre, Department of Physics, St. Xavier's College (Autonomous), Palayamkottai, Tamilnadu, India

²Department of Physics, St. Xavier's College (Autonomous), Palayamkottai, Tamilnadu, India
(Affiliated to Manonmaniam Sundaranar University, Abishekapatti, Tirunelveli, Tamilnadu, India)

*Corresponding author: gershomjeba@gmail.com

Received: 23-05-2022; Revised: 13-07-2022; Accepted: 14-07-2022; Published: 31-07-2022

© Creative Commons Attribution-NonCommercial-NoDerivatives 4.0 International License <https://doi.org/10.55218/JASR.202213610>

ABSTRACT

Rubidium sulfate crystal is an inorganic material and it is doped with an organic material viz. L-leucine to improve the various properties of the host crystal. L-leucine doped rubidium sulfate (LLRS) crystals have been grown by solution method. LLRS crystals have been harvested after the growth period of 30 days. The grown LLRS crystal is observed to be crystallizing in orthorhombic structure by single crystal XRD studies. Mechanical studies were carried out to find the mechanical strength and other parameters. Dielectric studies of L-leucine doped rubidium sulfate crystals were carried out to evaluate dielectric constant, dielectric loss and activation energy. UV-visible-NIR spectral studies were done in the wavelength range 200-1100 nm and linear optical properties like transmittance, absorption coefficient and extinction coefficient of samples have been evaluated. Second order Non Linear Optical (NLO) studies of the grown crystal of LLRS were carried out by Kurtz-Perry technique. The fundamental absorption was noted at 280 nm and at 278 nm for undoped and L-leucine doped rubidium sulphate crystals respectively. The optical band gap of LLRS crystal was found to be slightly more than that of undoped rubidium sulphate crystal. The SHG efficiency of LLRS crystal is observed to be 0.61 times that of the reference KDP sample.

Keywords: Inorganic Single Crystal, Mechanical Properties, Dielectric properties, NLO Properties.

1. INTRODUCTION

Amino acids like L-leucine, L-alanine, L-proline etc. have specific properties such as molecular chirality, which secures acentric crystallographic structures, absence of strongly conjugated bonds leading to high transparency ranges in the visible and UV spectral regions and zwitterionic nature of the molecule, which favours crystal hardness [1-3]. It is reported in the literature that L-leucine has been combined with nitric acid, oxalic acid, per chloric acid and picric acid to form many compounds and they are found to be useful NLO materials [4, 5]. Najar *et al.* have grown and studied rubidium sulfate complex crystal like lithium rubidium sulphate by slow evaporation technique. Single crystal X-ray diffraction analysis shows that the crystal belongs to a monoclinic system and some physical parameters like plasma energy, Penn gap, Fermi energy and electronic polarizability have been evaluated for the

grown crystal. From Vickers hardness test, the mechanical strength, and other parameters have been calculated [6]. Like lithium rubidium sulfate, many complex crystals have been studied and reported in the literature [7-11]. Many researchers carried out various studies of NLO crystals doped with impurities [12-14]. The impurity effect depends on the impurity concentration, supersaturation, temperature and pH of the solution. The effect of impurities on the growth rate and habit of the crystals growing in the solution has been the subject of many experimental and theoretical studies [15, 16]. In this work, L-leucine, an organic material, has been added into an inorganic crystal viz. rubidium sulfate to alter its physical and chemical properties. L-leucine is an essential amino acid and it has been grown and studied by Soma Adhikari *et al.* [17]. The novelty of the research is to grow L-leucine doped rubidium sulfate crystal by slow evaporation solution growth

technique first of its time and to report its various characterizations. In this work the authors' idea is to increase the growth rate of the L-leucine doped rubidium sulfate crystal and to enhance the mechanical properties of the material [18].

2. MATERIAL AND METHODS

High purity AR grade L-leucine was purchased commercially from Merck India. The Chemical Abstracts Service (CAS) number of L-leucine is 61-90-5. Rubidium sulfate was purchased commercially from sigma Aldrich. The purity is 99.8%. CAS number is 7488-54-2. Initially, saturated solution was prepared using rubidium sulfate and double distilled water and 1 mole% of L-leucine was added into the solution. The solution was stirred for about 4 hours using a hot plate magnetic stirrer and during the stirring the hotplate was switched on and it was maintained at temperature of 50°C. The solution was then cooled to room temperature and it was filtered using the good quality Whatmann filter paper. Slightly hot solution was kept in broad glass vessel and after 4 or 5 days, transparent seed crystals were obtained. Again the saturated solutions of the reactants were prepared in a beaker and some good quality seed crystals were placed at the bottom of the beaker covered with a perforated sheet. Due to slow evaporation, the seed crystals were turned into big-sized crystals after the growth period of 30 days.

3. RESULTS AND DISCUSSION

3.1. Finding the crystal structure and lattice parameters

X-ray diffraction (XRD) method is used to find the lattice parameters and hence the crystal structure. There are two XRD methods namely powder XRD method and single crystal XRD method to find the crystal structure. Since the sample is a single crystal, single crystal XRD method was adopted to solve the crystal structure. Single crystal X-ray diffractometer collects crystallographic data required for structure determination. The grown LLRS crystal was subjected to single crystal X-ray diffraction study at room temperature with $\text{MoK}\alpha$ radiation ($\lambda = 0.71073 \text{ \AA}$) using Bruker-Nonius MACH3/CAD4 diffractometer and the structural data were obtained. The units of the measurements for lattice parameters are in \AA and the angles in degree. The obtained single crystal XRD data for L-leucine doped rubidium sulfate (LLRS) crystal are presented in table 1. From the obtained data, it is observed that LLRS crystal belongs to orthorhombic system. For comparison purpose, the lattice parameters of undoped rubidium sulfate crystal were also found and the data are provided in the same table. When we compare the data, the crystal structure of undoped and L-leucine doped rubidium sulfate crystals are the same and due to doping of L-leucine into the lattice of rubidium sulfate crystal, the crystal structure does not altered.

Table 1: XRD data of undoped rubidium sulfate and L-leucine doped rubidium Sulfate (LLRS) crystals

Sample	Parameters (\AA)			Unit cell volume (\AA^3)	α°	β°	γ°
	a	b	c				
Undoped rubidium sulfate crystal	7.808 (3) \AA	5.959 (4) \AA	10.392 (2) \AA	483.52(3)	90	90	90
LLRS crystal	7.791 (2) \AA	5.963 (5) \AA	10.411 (4) \AA	484.05(2)	90	90	90

3.2. Dielectric properties

Dielectric properties like dielectric constant and dielectric loss of LLRS crystal were measured by using an LCR meter at different frequencies and temperatures. Jognic's LCR Meter (Model: 2816B) was used for the analysis. These properties are correlated with electro-optic property. The polished single crystal of LLRS was electroded on either side with graphite coating to make it behave like a parallel plate capacitor. Measurements were carried out two times to ascertain the correctness of the observed results. The dielectric constant of the crystal was calculated using the relation

$\epsilon_r = C/C_0$, where C is the capacitance of the capacitor in the presence of the crystal and C_0 is the capacitance in air. The measurement of dielectric constant and loss as a function of frequency and temperature gives the ideas of electrical processes that are taking place in materials. The variations of dielectric constant and dielectric loss for undoped and L-leucine doped rubidium sulfate crystal with frequency at room temperature are shown in the figs. 1 and 2. From the data, the dielectric parameters are found to decrease with increase in frequency. The high values of dielectric constant at low frequencies may be due to presence of all the four

polarizations namely, space charge, orientational, ionic and electronic polarizations and its low value at high frequencies may be due to the loss of significance of these polarizations gradually. In accordance with Miller’s rule, the lower value of dielectric constant at higher frequencies is a suitable parameter for the enhancement of SHG coefficient. The low value of dielectric loss at high frequency reveals the high optical quality of the crystal with lesser defects, which is the desirable property for NLO applications [19]. The variations of dielectric constant and dielectric loss for L-leucine doped rubidium sulfate crystal at different frequencies and temperatures are depicted in the figs.3 and 4. It is noticed that the dielectric constant and dielectric loss factor increase when the temperature of the samples increases.

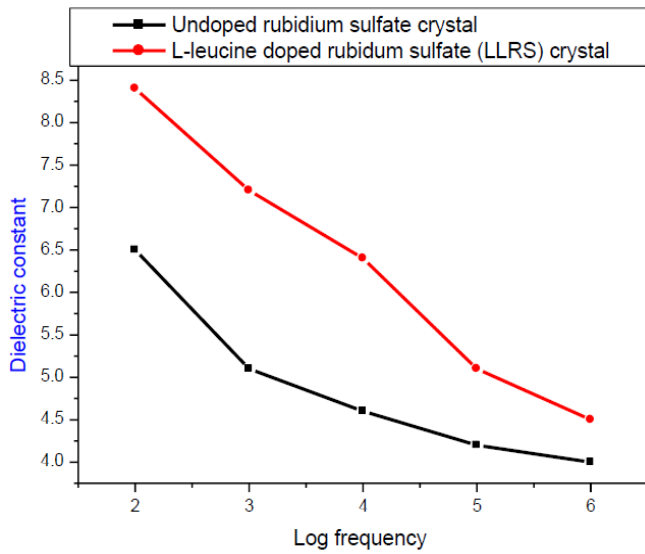


Fig. 1: Variation of dielectric constant for undoped and L-leucine doped rubidium sulfate crystal with frequency at room temperature (30°C)

The AC conductivity(σ_{ac}) was calculated using the relation $\sigma_{ac} = 2\pi f \epsilon_0 \epsilon_r \tan \delta$, where f is the frequency of the AC supply, ϵ_0 is the permittivity of free space or vacuum (8.852×10^{-12} F/m), ϵ_r is the relative permittivity or dielectric constant and $\tan \delta$ is the dissipation factor or dielectric loss. The calculated values of AC conductivity for LLRS crystal are given in the figs.5 and 6. From the results, it is observed that AC conductivity increases with increase of temperature of the sample and this is due to excitation of charged carriers from valence band to conduction band when the

temperature is increased. For many substances, as the temperature increases more and more defects are produced which, in turn, increase the conductivity. The defect concentration will increase exponentially with temperature and consequently the electrical conduction also increases. Also the added L-leucine into the lattice of LLRS crystal will act as the defect and conductivity increases with temperature [20].

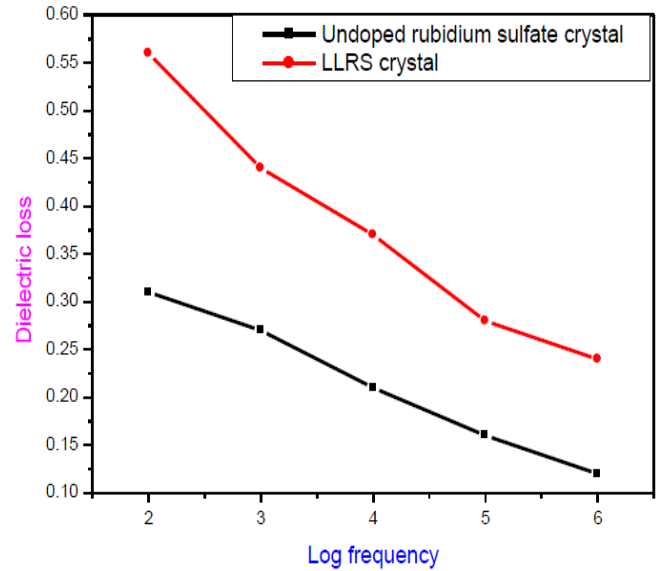


Fig. 2: Variation of dielectric loss for undoped and L-leucine doped rubidium sulfate crystal with frequency at room temperature (30°C)

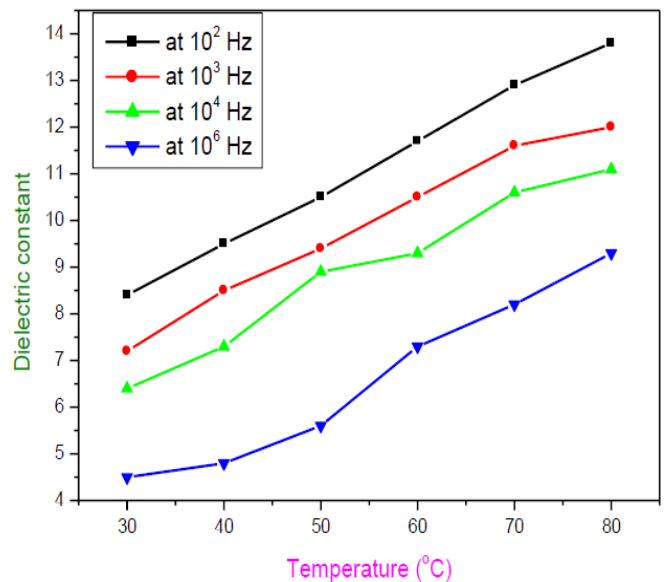


Fig. 3: Variation of dielectric constant for L-leucine doped rubidium sulfate crystal at different frequencies and temperatures

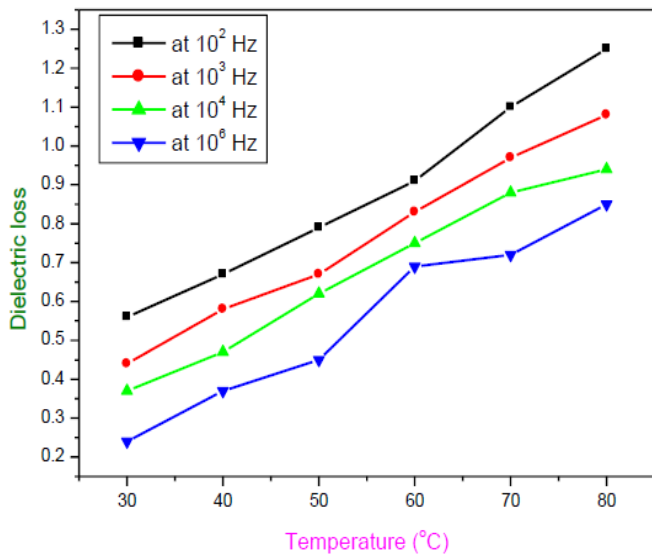


Fig. 4: Variation of dielectric loss for L-leucine doped rubidium sulfate crystal at different frequencies and temperatures

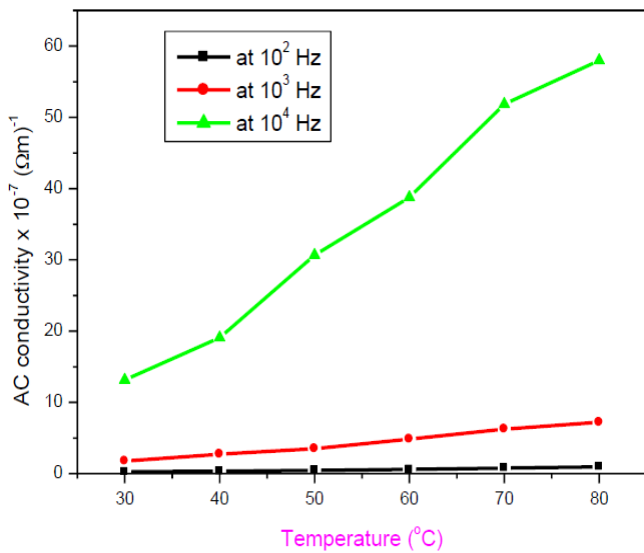


Fig. 5: Temperature dependence AC conductivity for L-leucine doped rubidium sulfate crystal at 10² Hz, 10³ Hz and 10⁴ Hz

AC conductivity (σ_{ac}) of the sample obeys the Arrhenius relation and the Arrhenius relation for a dielectric or insulating material is given by $\sigma_{ac} = \sigma_o \exp (-E/ kT)$ where σ_o is the pre-exponential factor, E is the activation energy for the AC conduction process and k is the Boltzmann's constant. By taking natural logarithm on both sides of the Arrhenius relation, the obtained expression is $\ln (\sigma_{ac}) = \ln (\sigma_o) - E/ kT$ and this is an equation of the straight line. By finding slope value, the

value of activation energy (E) can be obtained. For finding the values of slopes at different frequencies, the plots of $\ln (\sigma_{ac})$ versus $1000/T$ were drawn and they are provided in the figures 7, 8, 9 and 10. Using the relation $E = \text{slope} * k$, the values of activation energy at different frequencies like 10² Hz, 10³ Hz, 10⁴ Hz and 10⁶ Hz are determined and the obtained values of activation energy for L-leucine doped rubidium sulfate (LLRS) crystal are given the table 2. From the results, it is seen that activation energy is increasing when the frequency increases [21].

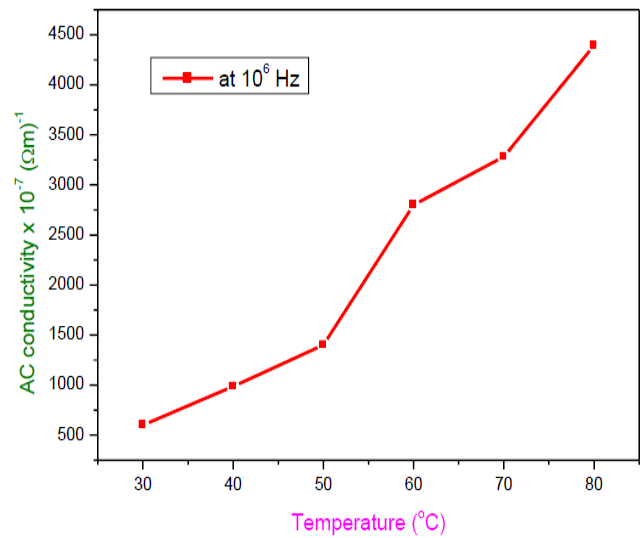


Fig. 6: Temperature dependence AC conductivity for L-leucine doped rubidium sulfate crystal at 10⁶ Hz

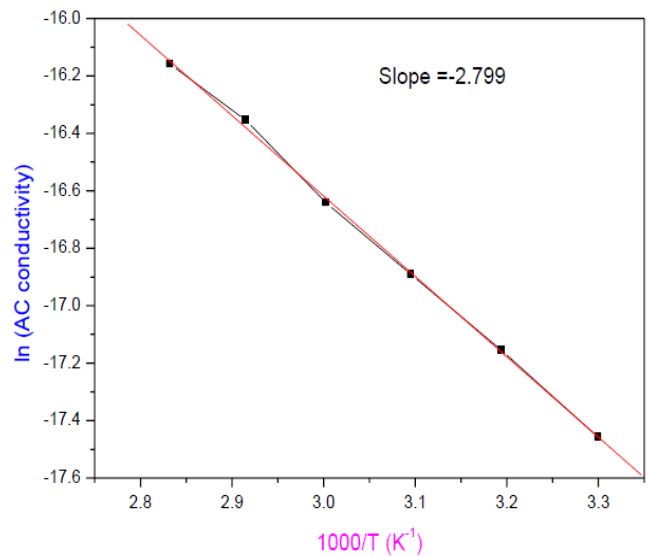


Fig. 7: Plot of $\ln (\text{AC conductivity})$ versus $1000/T$ for LLRS crystal at frequency of 10² Hz

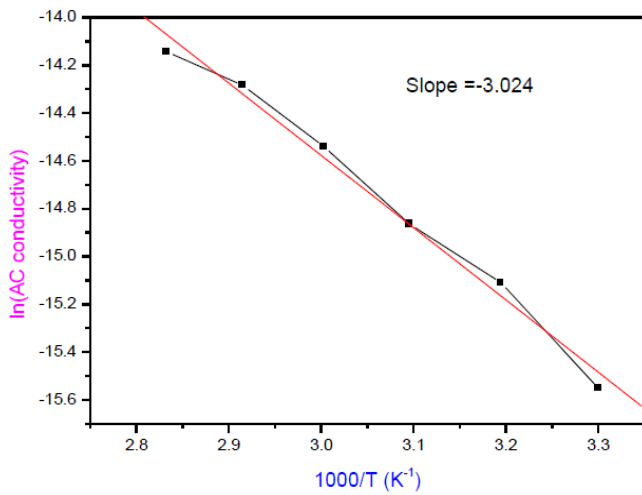


Fig. 8: Plot of ln (AC conductivity) versus 1000/T for LLRS crystal at frequency of 10³ Hz

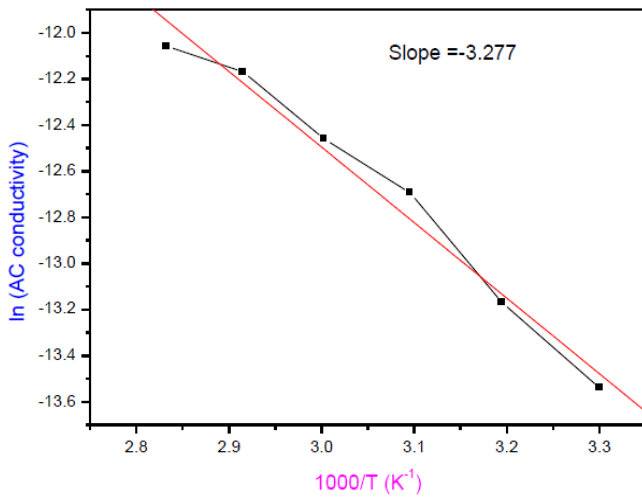


Fig. 9: Plot of ln (AC conductivity) versus 1000/T for LLRS crystal at frequency of 10⁴ Hz

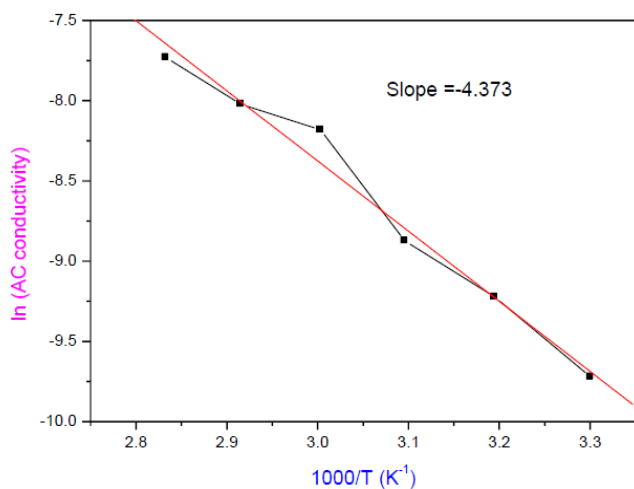


Fig. 10: Plot of ln (AC conductivity) versus 1000/T for LLRS crystal at frequency of 10⁶ Hz

Table 2: Values of activation energy for LLRS crystal at various frequencies

Frequency (Hz)	Activation energy (eV)
10 ²	0.242
10 ³	0.261
10 ⁴	0.283
10 ⁶	0.377

3.3. Measurement of SHG

Nonlinear optics is a new process in which light of one wavelength is converted to light of another wavelength and the creation of light of new wavelength is due to the electrons in nonlinear crystals. At high fields, polarization becomes independent of the field and the susceptibility becomes field dependent. Therefore, this nonlinear response is expressed by writing the induced polarization as a power series in the field.

$$P = \epsilon_0 \chi^{(1)} E + \chi^{(2)} E \cdot E + \chi^{(3)} E \cdot E \cdot E + \dots$$

In the above expression, $\chi^{(1)}$ is the linear term responsible for material's linear optical properties like, refractive index, dispersion, birefringence and absorption. $\chi^{(2)}$ is the quadratic term which describes second order NLO effects like second harmonic generation (SHG) in non-centrosymmetric materials. $\chi^{(3)}$ is the cubic term responsible for third harmonic generation, stimulated Raman scattering, phase conjugation and optical bistability. Measurement of SHG for undoped and L-leucine doped rubidium sulphate (LLRS) crystals was carried out by Kurtz and Perry test [22]. The powdered sample was illuminated using the Nd: YAG laser using the first harmonics output of 1064 nm with pulse width of 8ns and repetition rate 10 Hz. From the study, it is confirmed that there is no green laser light emission from undoped rubidium sulfate crystal. But it is observed that green laser light emitted from LLRS crystal when it was irradiated with Nd: YAG laser. Here potassium dihydrogen phosphate (KDP) crystal was used as the reference material. The result indicates that the relative SHG efficiency of LLRS crystal is 0.61 times that of KDP. Hence LLRS crystal is better than undoped rubidium sulfate crystal as far as the NLO applications are concerned.

3.4. UV-visible spectral studies

In UV-visible spectroscopy, the electrons involved are usually the valence or the bonding electrons, which can be excited by absorption of UV or visible or near IR

radiation. The quantity of absorption depends on the wavelength of the radiation and the structure of the compound. The radiation absorption is due to the subtraction of energy from the radiation beam when electrons in orbitals of lower energy are excited into orbitals of higher energy. After the sample absorbs a portion of the incident radiation, the remainder is transmitted on to a detector where it is changed into an electrical signal and displayed after amplification. The transmission spectrum shows what percentage of the incoming light that actually makes it through the sample. UV-visible spectrum gives information about the structure of the molecule, because the absorption of UV and visible light involves promotion of the electron in the σ and π orbital from the ground state to higher states. The UV-visible spectrum of LLRS crystal was recorded using Perkin Elmer Lambda 35 UV-Visible spectrophotometer in the wave length range 109-1100 nm and the spectrum is shown in fig.11. For comparison purpose, the spectrum of undoped rubidium sulfate crystal has also been recorded and it is shown in the same fig.11.

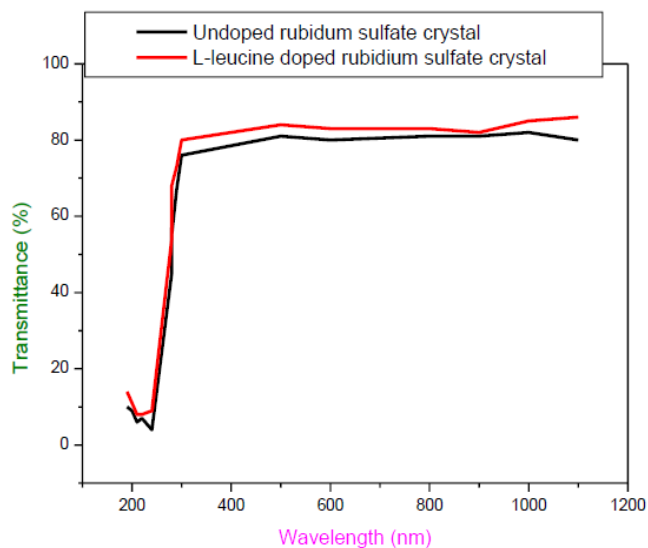


Fig. 11: UV-visible spectra of undoped and L-leucine doped Rubidium sulfate crystals

From the UV-visible transmission spectra, it is observed that both undoped and L-leucine doped rubidium sulfate crystals have high transmittance in the visible region and hence they have a wide optical transmission window. The UV cut-off wavelength values are observed to be at 280 nm and 278 nm respectively for undoped and L-leucine doped rubidium sulfate crystals. This observation ascertains the fact that the crystals can

be used for laser applications.

The measured transmittance (T) was used to calculate the absorption coefficient (α) using the formula:

$$\alpha = \frac{2.303}{t} \log\left(\frac{1}{T}\right)$$

Where 't' is the thickness of the sample.

The plots of absorption coefficient versus wavelength for both the samples are shown in the fig.12. The result indicates that the absorption coefficients of the samples are low in the visible region.

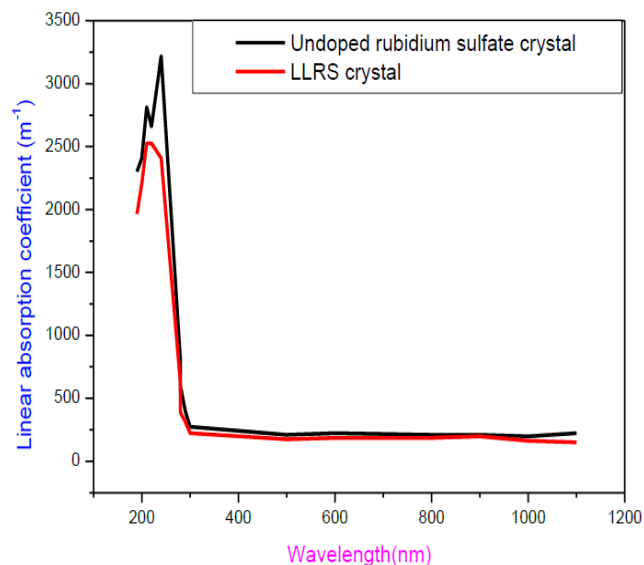


Fig. 12: Plots of absorption coefficient versus wavelength for undoped and L-leucine doped rubidium sulfate (LLRS) crystals

The dependence of optical absorption coefficient on photon energy is used to study the band structure and the type of transition electrons. The optical band gap was evaluated from the transmission spectra and the optical absorption coefficient α near the absorption edge is given by

$$\alpha = \frac{A(h\nu - E_g)^n}{h\nu}$$

Where E_g is the optical band gap of the crystal and A is a constant. For a direct transition $n = 1/2$ depending on whether the transition is allowed in quantum mechanical sense. The plots of $(\alpha h\nu)^2$ versus $h\nu$ (Tauc's plot) are shown in fig.13. The band gap was evaluated by the extrapolation of the linear part to the energy axis and its value is found to be 4.43eV for undoped rubidium sulfate crystal and for L-leucine doped rubidium sulfate (LLRS) crystal, the optical band gap is 4.48 eV. Hence, the band gap of LLRS crystal is slightly more than that of

undoped rubidium sulfate crystal. The extinction coefficient (K) can be obtained from the following relation:

$$K = \frac{\lambda\alpha}{4\pi}$$

The extinction coefficients as a function of wavelength for both the samples are presented in the fig.14. It is observed that extinction coefficient of the samples is high at cut-off wavelength and it is found to be increasing with increase of wavelength in the visible region [23-25].

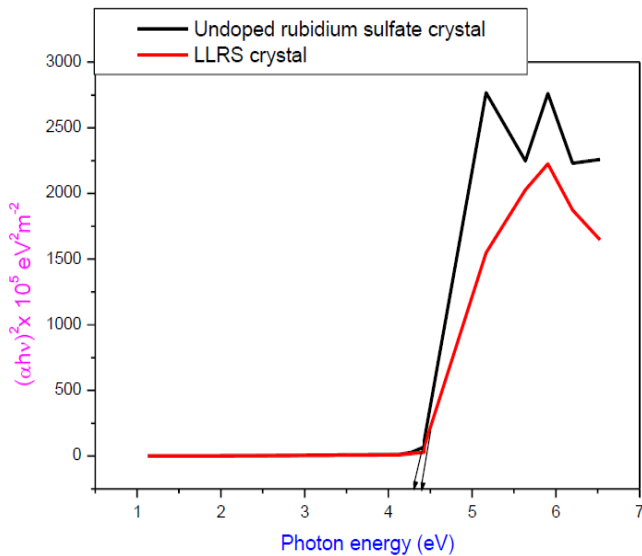


Fig. 13: Tauc's plots for undoped and L-leucine doped rubidium sulfate crystals

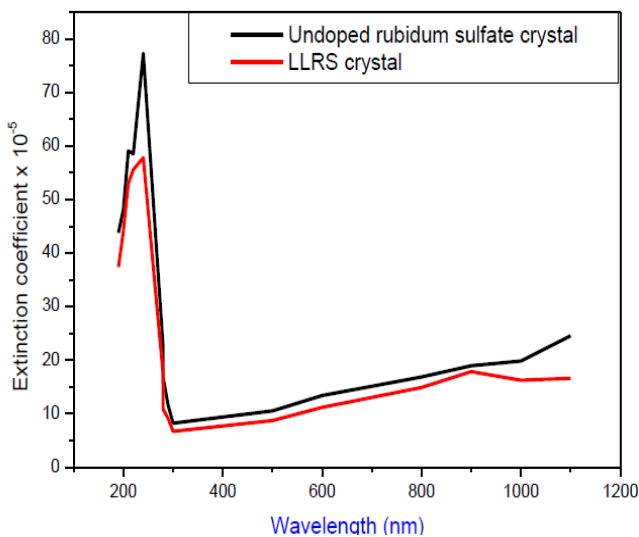


Fig. 14: Variation of extinction coefficient with wavelength for undoped and L-leucine doped rubidium sulfate (LLRS) crystals

3.5. Micro hardness, stiffness constant and yield strength

The micro hardness of the sample was measured by using the Shimadzu (Model: HMV-2T) Vickers micro hardness tester. In this experiment, a pyramidal indenter was used. By applying loads, the average diagonal indentation was measured and using these values, the micro hardness number was determined. Using the values of average diagonal indentation, the micro hardness number (H_v) of the undoped and L-leucine doped rubidium sulfate (LLRS) crystals was calculated using the formula $H_v = 1.8544 \times P / d^2$ where, P is the applied load and d is the diagonal length of indentation. The plots of micro hardness versus applied load for both the crystals are shown in the fig.15. It is observed that the hardness increases with increase of the applied load for both the samples and this is due to reverse indentation size effect.

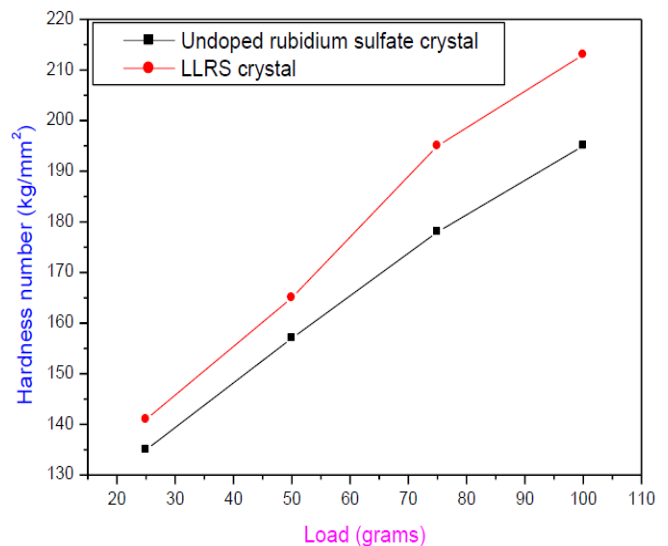


Fig. 15: Plots of micro hardness number versus applied load for undoped and L-leucine doped rubidium sulfate (LLRS) crystals

Yield strength is defined as the maximum stress that can be developed in a material without causing plastic deformation and it is also called as the yield stress. It is related to the yield point and it is the point on the stress-strain curve that indicates the limit of elastic behavior and the beginning of plastic behavior. Prior to the yield point the material will deform elastically and will return to its original shape when the applied stress is removed. Once the yield point is passed, some fraction of the deformation will be permanent and non-reversible. Yield strength depends on micro hardness

(H_v) and the relation used for calculating the yield strength is (σ_y) = ($H_v/3$). Another mechanical property viz., stiffness constant (C_{11}) is determined using the relation $C_{11} = H_v^{7/4}$ where, H_v is the micro hardness of the sample. The calculated values of yield strength for both the samples are provided in the table 3. From the data, it is observed that both yield strength and stiffness constant of the samples are high these values are increasing with increase of applied load. The values of stiffness constant of the samples are given in the table 4. Stiffness constant of the samples also increases as the load increases. Since hardness, yield strength and stiffness constant of undoped and L-leucine doped rubidium sulfate (LLRS) crystals are high, these crystals can be used for NLO device fabrication [26-29].

Table 3: Values of yield strength for undoped and L-leucine doped rubidium sulfate (LLRS) crystals

Load (grams)	Yield strength (Mega pascal)	
	Undoped rubidium sulphate crystal	LLRS crystal
25	441.01	460.62
50	512.86	539.42
76	581.46	637.11
100	637.10	695.83

Table 4: Values of stiffness constant for undoped and L-leucine doped rubidium sulfate crystals

Load (grams)	Stiffness constant (pascal)	
	Undoped rubidium sulphate crystal	LLRS crystal
25	9.17761E+15	9.90328E+15
50	1.19528E+16	1.30389E+16
76	1.48895E+16	1.74665E+16
100	1.74665E+16	2.0385E+16

4. CONCLUSION

L-leucine has been added into the lattice of rubidium sulphate crystal to alter its properties. Aqueous solution growth method was adopted to grow the single crystals of L-leucine doped rubidium sulphate (LLRS). The crystal structure of the grown LLRS crystal was found to be orthorhombic. It is observed that doping of L-leucine into rubidium sulphate crystal does not change the crystal structure. Dielectric properties like dielectric constant and dielectric loss of the sample were measured at various frequencies and temperatures and activation energy was determined.

The fundamental absorption was noted at 280 nm and at 278 nm for undoped and L-leucine doped rubidium sulphate crystals respectively. The optical band gap of LLRS crystal was found to be slightly more than that of undoped rubidium sulphate crystal. The SHG efficiency of LLRS crystal is observed to be 0.61 times that of the reference KDP sample. The mechanical properties like hardness, yield strength and stiffness constant of both undoped and L-leucine doped rubidium sulphate crystals have been determined. This present study will be helpful to the researchers to grow various rubidium sulphate based Non Linear Optical crystals in future. Further researches shall also be conducted on the same crystal by changing the method of crystal growth like Sankaranarayanan-Ramasamy method.

5. ACKNOWLEDGMENT

The authors are thankful to the staff members of St. Joseph's college, Trichy, Cochin University, Cochin and Crescent Engineering College, Chennai for the research support to carry out this investigation.

Declaration of competing interest

The authors declare that they have no known competing financial interests or personal relationships that could have appeared to influence the work reported in this research paper

6. REFERENCES

- Xing G, Jiang M, Zishao X, Xu D. *Chin. J. Lasers*, 1987; 14:357-365.
- Versko S, *Laser Program Annual Report, Lawrence UCRL-JC 105000*; Lawrence Livermore National Laboratory, Livermore, CA, USA, 1990.
- Warren LF, Proceedings of the Fourth International Sample Electronics Society for the Advancement of Materials and Process Engineering of Materials and Process Engineering, Covina, CA, USA, 1990; Allred RE, Martinez RJ, Wischmann KB. Eds, 1990; 4:388.
- Adhikari S, Kar T. *J. Cryst. Growth*, 2012; 356:4-9.
- Anbuezhayan M, Ponnusamy S, Muthamizhchelvan C. *J. Optoelectron. Adv. Mater.*, 2009; 3:1161-1167.
- Najar A, Vakil GB, Wanty B. *J. Adv. Dielectr.*, 2018; 8:1-11.
- Fonseca CHA, Ribeiro GM, Gazzinelli RT, Chaves AS. *Solid State Commun.*, 1983; 46:221-225.

8. Ahmed MA, Hiti MA, Nimr MK, Kassem ME. *J. Mater. Sci. Lett.*, 1992; **11**:1109-1112.
9. Liu QG, Worrell WL. *Solid State Ion*, 1986; **18**:524-528.
10. Shiroishi Y, Nakata A, Sawada S. *J. Phys. Soc. Jpn.* 1976; **40**:911-912.
11. Podder J. *J. Cryst. Growth*, 2002; **237**:70-75.
12. Podder J, Ramalingom S, Kalkura SN. *Cryst. Res. Technol.*, 2001; **36**:549-551.
13. Li G, Liping X, Su G, Zhuang X, Li Z, He Y. *J. Cryst. Growth*, 2005; **274**:555-562.
14. Sangwal K. *Prog. Cryst. Growth Charact. Mater.*, 1996; **32**:3-43.
15. Freeda TH, Mahadevan C. *Bull. Mater. Sci.*, 2000; **23**:335-340.
16. Rao KV, Samakula A, *J. Appl. Physics*, 1995; **36**:2031-2038.
17. Adhikari S, Kar T. *Mater. Chem. Physics*, 2012; **133**: 1055-1059.
18. Hojjati Najafabadi A, Mozaffarinia R, Rahimi H, Shoja Razavi R, Paimozd E. *Surface Engineering*, 2013; **29**:249-254.
19. Rose AS, Selvarajan P, Perumal S. *Spectrochim. Acta A*, 2011; **481**:270-275.
20. Tareev B, *Physics of Dielectric Materials*, Mir Publishers: Moscow, Russia, 1979.
21. Selvarajan P, Das BN, Gon HB, Rao KV. *J. Mater. Science*, 1994; **29**:4061-4064.
22. Kurtz SK, Perry TT. *J. Appl. Phys*, 1968; **39**:3798-3813.
23. Armstrong JA, Bloembergen N, Ducuing J, Pershan PS. *Phys. Rev.*, 1962; **127**:1918-1939.
24. Xue D, Ratajczak H. *Chem. Phys. Lett.*, 2003; **371**:601-607.
25. Park H, Kim TK, Cho SW, Jang HS, Lee S, Choi SY. *Sci. Rep.*, 2017; **7**:1-8.
26. Hanumantharao R, Bhagavannarayana G, Kalainathan S. *Spectrochim. Acta A*, 2012; **91**:345-351.
27. Chandler H, *Hardness Testing*; ASM International: New York, NY, USA, 1999.
28. Raj KR, Murugakoothan P. *Optik*, 2013; **124**:2696-2700.
29. El-Fadl AA, Soltan AS, Shaalan NM, *Cryst. Res. Technol.*, 2007; **42**:364-377.